Impact of Waste Disposal Site on Groundwater Quality at Rafin-Tofa Dumpsite, Kampala, Niger State, Nigeria

SHEHU ATABO IBRAHIM
Force Education Unit, Police Secondary School, Minna, Niger State – Nigeria.

Abstract- ***The impact of waste disposal site on groundwater quality at Rafin-Tofa dumpsite, Kampala, Niger State, Nigeria was investigated using 2D Electrical Resistivity Imaging (ERI) and Vertical Electrical Sounding (VES). Resistivity data were collected from parallel survey of 9 profile lines at the dumpsite and 3 control profile lines using a Wenner-Alpha array configuration. The 2-D results revealed three distinct lithology which includes topsoil, weathered basement and fresh basement. The topsoil comprises of clay, lateritic soil, and peat/clay materials. The 2-D resistivity values 2.31-40.0 Ωm at profile distance 0.0-100 m at the depths 1.25-12.4 m across various profiles were interpreted as contaminated zone which also correspond to VES 5, 6, 8 and 9. High resistivity values range from 889-7823.4 Ωm at the depth 7-14.5 m correspond to VES results at profiles 1,2,3,4 and 7 was interpreted as weathered basement rock. The 2-D results of the control sites which constitute profiles 10, 11 and 12 revealed the resistivity values that range from 88.2-482 Ωm from profiles distance 0.0-100 m at the depth of 1.25- 19.8 m across various profiles was interpreted as weathered rock which is free from contamination. The results of the control sites indicate that the layer is underlain by clay lithology. The 2-D ERI and VES sections of the model resolved clearly the subsurface lithological variations. Interpretation of the field data showed that 2-D ERI and VES techniques were effective in delineating groundwater contaminated zones. The vertical and horizontal sensitivity of the 2-D Wenner-Alpha array for sub- surface resistivity variations made it possible to determine the position and extent of leachate infiltration into groundwater. It can be deduced from 2-D and VES results that the area associated with low resistivity is prone to leachate penetration and as such hand dug well is not safe for consumption. Level of leachate contamination of the subsurface was observed on the entire sites at varying depths. The impact of waste disposal site is that; the study was able to delineate the depth of the contamination of the area to be at 9.25 m. This depth indicates that any borehole to be drilled at that area must be beyond the depth of 10.00 m to avoid infiltration 0f contaminant to the water.***

I. INTRODUCTION

1.1 Background to the Study

Groundwater is the major sources of drinking water in semi-arid region of Nigeria. Its quality is mostly compromised in towns and cities due to increase human activities which has led to the production of large tones of solid waste materials daily and they are poorly disposed. The importance of groundwater as a valuable source of portable water cannot be over emphasized. Groundwater forms the most important natural resources of any region and compliments surface sources in the position of portable water for domestics and industrial applications. A leachate is any liquid in the cause of passing through matter, extracts soluble or suspended solids, or any other component of the material through which it has passed. Leachate released into groundwater may cause severe risks to human health and the environment. Groundwater is a source for boreholes, and boreholes are the main source of domestic water in many areas of Nigeria. They depend on it for both local and commercial purposes; therefore, its contamination is a direct threat to the health of the residents of an affected community. Medical literature tells us that some general health conditions caused by consuming leachate contaminated water can range from sweating, bleeding, stomach disorders, blood disorders, congenital disabilities and even cancer. However, based on the different hazardous components of these leachates, the effects vary (Amah, 2020).

Groundwater contamination (also called groundwater pollution) occurs when pollutants are released to the ground and they make their way into groundwater. The pollutants often create a contaminant plume within an aquifer. Movement of water and dispersion within the aquifer spreads the pollutants over a wider area. Groundwater pollution due to leachate infiltration into the subsurface has been on the rise in recent times, due to the production of large amount of solid waste through domestics, agriculture and industrial processes. Leachate released into groundwater may also cause danger to the environment by enhancing the growth of toxic substances. Groundwater is recharged and eventually flows to the surface naturally, natural discharge often occurs as springs. Groundwater constitutes 20% of

the world's fresh water supply (Alhassan *et al.*, 2017).

Underground water is the water present beneath the earth's surface, found in soil pore spaces and the crevices of rock formations. It is highly useful and usually an abundant resources but overuse can cause depletion. One of the most evident problems, however, comes from natural or human induced contamination. Due to its liquid form and extremely high concentration, leachate can easily seep in through the soil and very small amount can pollute a large volume of groundwater, leaving it unsuitable for domestic use.

Any material that is discarded after its primary use is waste. Society produces different types of waste; domestic waste, industrial wastes, mining wastes and radioactive wastes (Ranke, 2001). Liquid or solid wastes, hazardous or non-hazardous wastes infiltrating into groundwater can cause some chemical reactions which may produce substances dangerous to environment and health (Ige, 2013). In the last decade the study area has witness a major increase in waste disposal on uncontrolled disposal sites. Waste disposal is an expensive urban environmental problem. The degradation of water quality is undesirable irrespective of whether it results directly from leachate escaping from the landfill or from geogenic processes (Amadi *et al*., 2017). Leachate is formed when rainwater and runoff percolate through solid waste, leaching out soluble salts and biodegraded organic products. Due to downward darcy velocity and diffusion, contaminants will migrate from the landfill through soil into the groundwater system (Franz, 1993).

Wastes, which are described here are materials that result from an activity or process, but have no immediate economic value or demand and must be discarded. In this area like in most other areas and cities, waste are generated daily and most of the waste are discarded at the dumpsites that are not engineered. This threatens the groundwater and road facilities not sparing the aesthetics of such affected area. During the peak of rainy season, dumpsites are covered by flood water and this contributes to the formation of the leachate (water that has percolated through waste and contains ions in solution). It is the contaminated liquid (leachate) that forms '' plume'' that moves outward and downward into the surrounding and underlying aquifers (Carpenter *et al.,* 2012).

These plumes may contain dissolved carcinogens such as heavy metals (e.g. lead, mercury, Chromium, Cadmium, Arsenic, etc.), Volatile Organic Compounds (VOCs) and ions (sodium, calcium, iron, sulphate, chloride, etc.). Some of these methods include magnetic, electrical resistivity, electromagnetic, gravity, seismic, remote sensing etc. In all, the electrical resistivity method has been the most widely used geophysical tool for groundwater contamination investigation because of its advantage which include simplicity in field technique and data handling procedure (Anomoharam, 2013) and it's the most effective (Alhassan *et al.,* 2017).

Observation of poor water quality in adjacent wells or boreholes are indicators that leachate is being produced and is moving. The direction of groundwater flow may not confirm to surface water flow direction. However, groundwater moves slowly and continuously through the open spaces in the soil and rock. If a dumpsite contaminates groundwater, a plume of contamination will occur. Wells in that plume will be contaminated, but other wells, even those close to the dumpsite may be unaffected if they are not in the plume (Taylor and Allen 2006).

When groundwater becomes polluted, the risk of surface water contamination also increase due to the interconnectivity between groundwater and surface water. Landfills have served many years as ultimate disposal site for all types of waste, municipal solid waste, industrial sewage and hazardous waste. Modern landfills have liners at the base, which acts as barriers to leachate migration. However, it is widely acknowledged that such liners deteriorate over time and ultimately fail to prevent the movement of leachate into an aquifer (Jagloo, 2002).

Water contamination either natural or anthropogenic is the major problem of water especially in developing countries. Once contaminated, water, especially groundwater may remain polluted without remedy or treatment. Water in its liquid form is the material that makes life possible on earth. All living organisms are composed of cells that contain at least 60% of water (Jackson, 1985).

Leachate is a liquid formed from the decomposition of waste and has high conductivity due to the

presence of dissolve salts. The electrical resistivity of the leachate is often very much lower than natural groundwater. Pollutants or contaminants released into the environment rarely remains at the point of discharge. They are transported through the porous soil by the process of absorption, advection, molecular diffusion and dispersion. Leachate is generally associated with high ion concentration and therefore rock formation contain in them is characterised with very low resistivity (Cristina *et al.,* 2012)

Leachate is mostly formed through the:

1. Biological decay of organic materials, either aerobically or anaerobically.
2. Chemical oxidation of waste materials.
3. Escape of gases from dumpsite.
4. Dissolving and leaching of organic and inorganic wastes by water and leachate moving through the dumpsite.
5. The flow of dissolved materials by concentration gradients and osmosis.

Immediately after solid waste material are deposited in dumpsite, the process of stabilization begins. This process, which forms the leachate within the site, occurs mainly through four key processes. These processes include hydrolyses of solid waste, biological degradation of organic waste, solubilisation of soluble salts contained within the waste mass and the transportation of waste as colloids or particular matter (Kjeldsen *et al.,* 2002).

Vertical Electrical Sounding (VES) is an electrical resistivity method that is widely used for depth sounding due to its simplicity and reliability (Olawuyi and Abolarin, 2013). Vertical Electrical Sounding (VES) is a geophysical method for investigation of geological medium. The method is based on the estimation of the electrical conductivity or resistivity of the medium.

The electrical resistivity method can be best employed to estimate the thickness of over burden and also the Electrical Profiling in a DC resistivity survey which aim to trace lateral variations in the apparent resistivity structure of the subsurface.

II. LOCATION OF THE STUDY AREA

The study area is located at Rafin-Tofa via Kampala, northern part of Bosso Local Government Area of Niger State. It lies between latitudes 9^0 40' 04" N, and 9^0 40' 35" N and longitudes 6^0 25' 48" E and 6^0 26' 45" E. The southern end of the area is bounded by Government Day Secondary School, Maikunkele and its northern part is behind the fish house which is about 100m away from Minna-Zungeru road. The terrain is relatively flat and accessible by road. This reflect in figure 1.2, 1.3 and plate 1. The rock types present in the area are part of granitic suite which are mostly exposed along the stream channels (Udensi *et al.,* 2005).

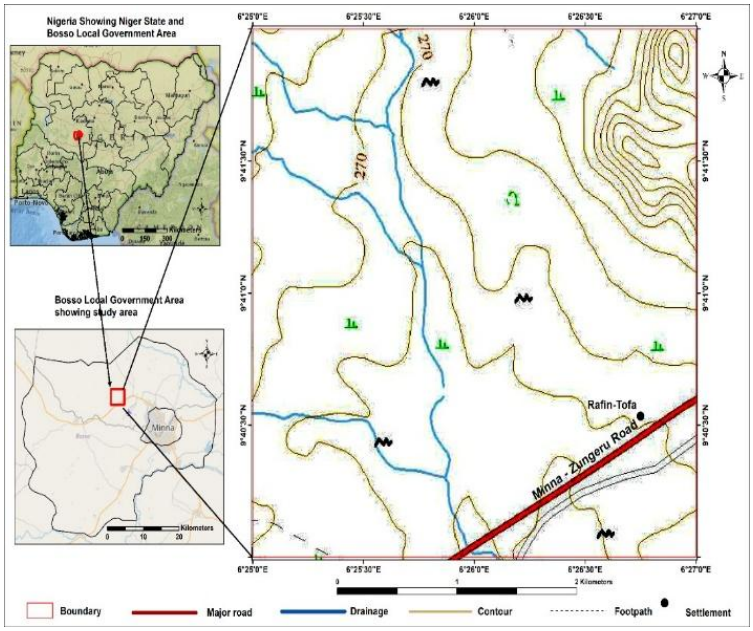

Figure 1: Location Map of the Study Area (Office of the Surveyor General of the Federation (OSGOF), 2010)

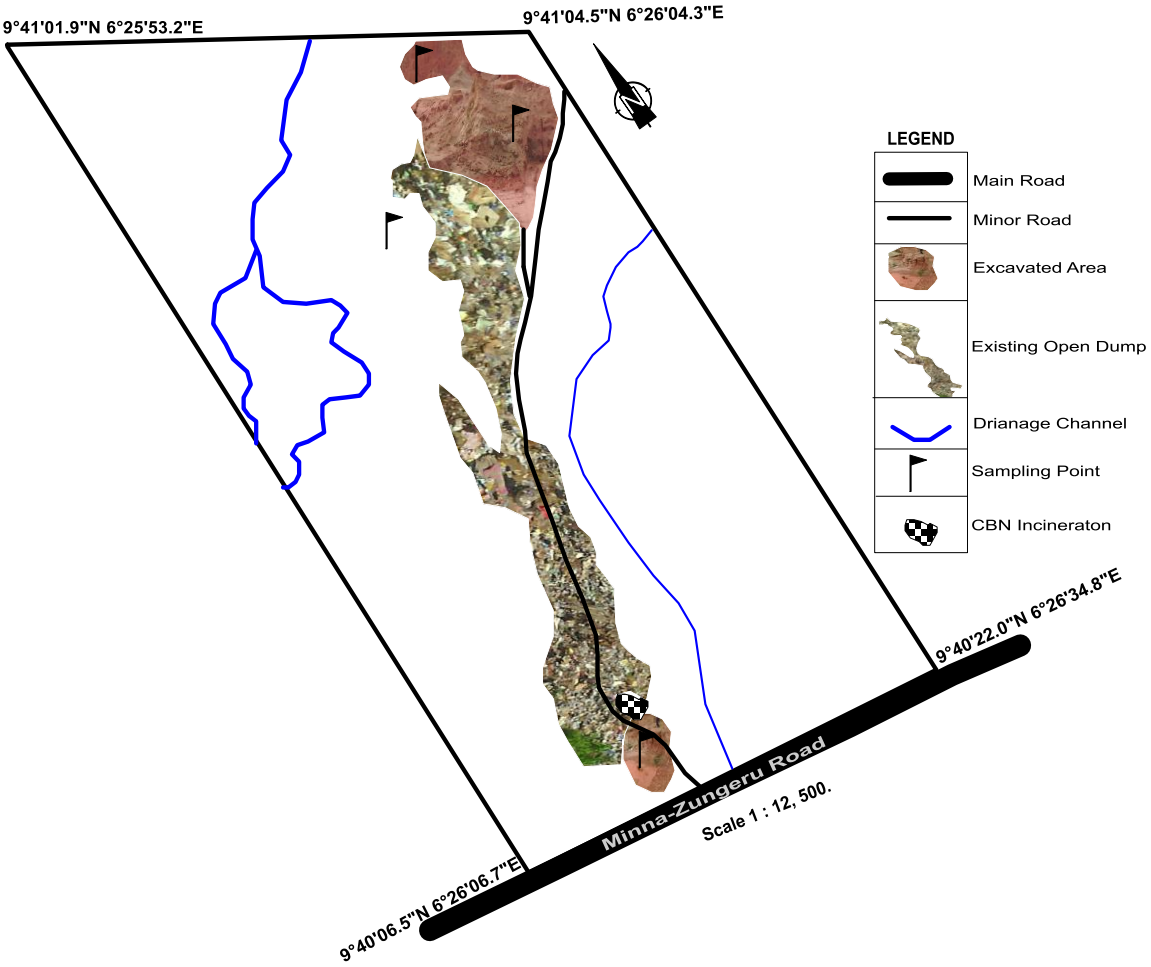

Figure 2: Study Area Location

Plate 1 shows Rafin-Tofa solid waste dumpsite where investigation on contamination of groundwater was carried out.

Plate 1: Rafin-Tofa Solid Waste Dumpsite.

III. MATERIALS AND METHOD

3.1 Materials

Instrumentation for Electrical Resistivity Survey

The equipment used for the resistivity method is reasonably cheap and easy to use. The resistivity field data were acquired with the aid of the following equipment:-

ABEM SAS 4000 Terameter - This is the major power source of the whole set-up. It measures the resistance of the subsurface layers and can also measure the voltage of the power source. The equipment has an in-built system of reducing the effect of noise. The instrument is portable and fixed with a rechargeable battery. It has a maximum power of 18 watts, manual selection of current in steps up to 100mA, a choice of sample time/ signal length averaged three frequency settings.

Electrodes- These are steel rods of about 30cm with a base and a pointed end. The pointed end is use to penetrate the ground. The material makes it a good conductor. Four electrodes were used; the first pair is the potential electrode while the second pair is the current electrode. Their basic function is to pass current into the ground and measure potential between two points. Two-third of the length of the electrodes was driven below the earth surface.

Cables- They are made of conducting material (copper). There were four reels of cables used during the geophysical survey. The cables are connected to the terameter on one end and the other is connected to the electrodes.

Clips- These are objects used for passing the currents from the cables to the electrodes by clipping the electrodes after wounding the cable on it. The mouth is made of conducting materials while the base (handle) is made of insulating material to prevent electrocution. The clips ensure good electrical contact.

Hammer and Cutlass-These were used to drive the electrodes into the ground. It consists of a relatively slim wooden cylindrical handle embedded into a metallic head. The cutlass was used to clear the path along which measurement are to be taken.

Tapes- These are used for making measurements of length on the field as they have been calibrated in metric units. The tape used is 100m in length. It was used in measuring electrode spacing on the field.

Global Positioning System and Compass-Clinometer- These equipments were used for taking coordinates and bearing. GPS was used for taking the longitudes, latitudes and elevation of various locations. It is portable and handy. The compass-clinometer was used to take direction of the profiles.

Field Stationery- These are writing materials that were used to record all observation and field data. The stationery consists of pencils, pens, recording sheets, rulers and so on.

3.2 Method

2D Electrical Resistivity Imaging (ERI) survey using a Wenner-Alpha array as outlined by Loke (1999) was conducted along twelve parallel profiles anda total of 12 VES points were sounded in both dump site and control site within the vicinity of the dumpsite. The selection of the ERI locations was dependent on the availability of areas free of heap of waste as an obstacle. When the conditions to enable the electrodes penetrate the natural soil was allowed, the roll-along technique was applied for getting continuous profile. The apparent resistivity measurements were acquired using ABEM SAS 4000 Terameter. A pre-defined sequence of combinations of four stainless steel electrodes with current electrodes (C_1 and C_2) and potential electrodes (P_1andP_2) for different electrode spacing (a) and data acquisitions levels (n) was adopted.

The profile length (L) of the electrical cable spread was restricted to 100m with a total of 21 electrodes on a profile line. At the initial series of measurement transverse the spacing in the middle of nearby electrodes (a) at 1a was set at 5m. For the initial measurement, electrodes numbers 1, 2, 3 and 4 represents C_1 , P_1 , P_2 and C_2 . For the following measurement, numbers electrodes 2, 3, 4, and 5 represented C_1 , P_1 , P_2 and C_2 in that order. This arrangement was sustained till electrodes numbers 18, 19, 20 and 21 represents C_1 , P_1 , P_2 and C_2 in turn. Eighteen mid-points were established for the first measurement sequence. The entire measurement technique was replicated for 2a, 3a, 4a, 5a, 6a etcetera. Beginning at the first series of measurement 1a, a total number of 18 mid-points were established, and the mid-point decreases by three in successively sequences measured. For a profile of 100m, at 2a,

mid-points =15, at 3a=12, 4a =9, 5a=6 and 6a=3 (Figure 3.1). The subsurface resistivity values acquired are arranged in apparent resistivity pseudo-sections which give a qualitative approximation of the subsurface resistivity distribution. An inversion procedure using the RES2DINV software ver. 3.71 (Loke, 1999) was used to generate 2D ERI sections from the apparent resistivity data. RES2DINV finite difference method based on the regularized least squares optimization procedure to produce 2D synthetic resistivity model is designed to discuss and validate the interpretation of the field data. The software iteratively determines the model blocks (Figure3) resistivity that will closely produce the measured apparent resistivity data (Loke, 1997).

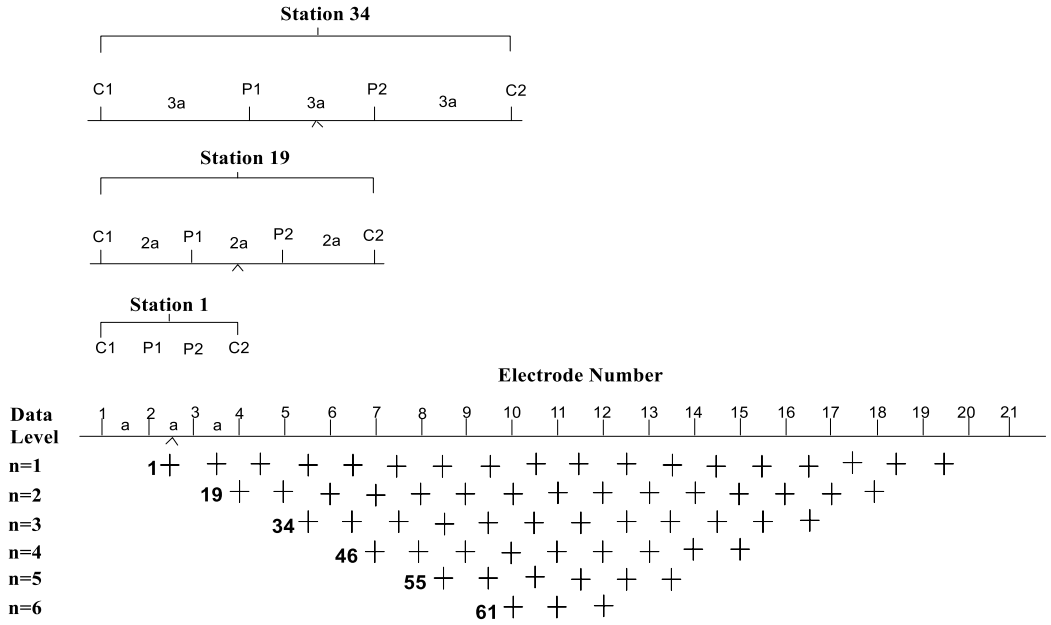

Figure 3 Sequence of 2D Wenner resistivity measurement to build a pseudosection (After Loke, 1999 and 2012).

Table 1: Range of Resistivity Values for Various Rock Types in Basement Complex Used in Driving the Geologic Sections. (Daniel *et al.*2011).

ROCK TYPE	RANGE OF RESISTIVITY (**Ω**m)
Granite	300 - 10^5
Clays	1 – 100
Gravel	100 – 1500
Alluvium and sand	10 – 800
Quartzite (various)	10 – 2 x 10^8
Weathered laterite	150 – 900
Fresh laterite	900 – 3500
Weathered basement	20 – 500
Fractured basement	500- 1000
Fresh basement	>1000

Table 2: Borehole Log around Minna Area

Depth(m)	Lithology	Description
0-0.5	Surficial Sand Deposit	Sandy Top Soil
0.5 – 3	Laterite and Clay	Red- Brown Lateritic Soil
3 – 4.5	Clay-Weathered Rock	Reddish to Brown Clay with Weathered Rock Material
4.5 -12	Weathered Rock (Granite)	Brown to Dark Brown Biotite Granite
12 – 35	Fractured Weathered Rock(Granite)	Dark Brown Biotite Granite

Table 1 and table 2 was used to interpret the result and discussion in chapter four

3.3 Theory of Electrical Resistivity Method

At each measurement, the resistivity meter displayed resistance value and associated root mean square error of the reading. The electrical resistivity tomography (ET) provides 2D information about the subsurface materials and depth. Twelve (12) vertical electrical resistivity sounding was carried out in the study area using Schlumberger array with the aim of delineating the depth to the groundwater, aquifer thickness and other physical parameters.

From Ohm's law

$$R = \frac{V}{I} \qquad (3.1)$$

where R is the resistance of a wire or material conductor measured in ohms (Ω), V is the voltage measured in volt (v), I is the current of the wire measured in ampere (A)

The resistivity of the earth material is determined by

$$\rho = \frac{RA}{L} \qquad (3.2)$$

where ρ is a constant of proportionality known as the resistivity of the earth material measured in ohms-meter(Ωm).

R is the resistance of a wire or material conductor measured in ohms (Ω). A its cross-sectional area measured in meter square (m^2) and L is the length measured in meter (m)

If we measure the potential difference between two shells at some distance D from the electrode, we get:

$$dv = IR = I\left(\rho\frac{L}{A}\right) = I\left(\rho\frac{dr}{2\pi r^2}\right) \qquad (3.3)$$

where dr is the thickness of the shell across which we measure the potential, recalling that the resistivity of air is so high, no current will flow through it, so we only need the surface of a hemisphere ($2\pi r^2$).

We now integrate from infinity (where potential is zero) to get the potential at a point distance D from the source:

$$V = \int_D^\infty dv = \frac{I\rho}{2\pi}\int_D^\infty \frac{dr}{r^2} = \frac{I\rho}{2\pi D} \qquad (3.4)$$

If the resistivity of the ground is uniform, the current, I, in equation 3.4 is the current in the wire, not the current in the ground, which varies. For two electrodes: If we move the other current electrode from far away, we can calculate the potential at point P_1 by just adding the potentials from both current electrodes, remembering that one is positive, and the other negative:

$$V_{P_1} = \frac{I\rho}{2\pi r_1} - \frac{I\rho}{2\pi r_2} = \frac{I\rho}{2\pi}\left(\frac{1}{r_1} - \frac{1}{r_2}\right) \qquad (3.5)$$

When we use the same argument by summing potentials to obtain the voltage across two electrodes, the potential difference between P_1 and P_2 is:

$$V_{P_1-P_2} = V_{P_1} - V_{P_2}$$
$$V_{P_1} = \left(V_{c_1} + V_{c_2}\right)_{P_1}$$
$$V_{P_2} = \left(V_{c_1} + V_{c_2}\right)_{P_2}$$

$$V_{P_1-P_2} = \left(\frac{I\rho}{2\pi r_1} - \frac{I\rho}{2\pi r_2}\right) - \left(\frac{I\rho}{2\pi r_3} - \frac{I\rho}{2\pi r_4}\right) = \frac{I\rho}{2\pi}\left(\frac{1}{r_1} - \frac{1}{r_2} - \frac{1}{r_3} + \frac{1}{r_4}\right) \qquad (3.6)$$

Where r_1, r_2, r_3 and r_4 are the distances between various electrodes.

Solving for the resistivity:

$$\rho = \frac{2\pi V_{P_1-P_2}}{I}\frac{1}{\frac{1}{r_1} - \frac{1}{r_2} - \frac{1}{r_3} + \frac{1}{r_4}}$$

$$\rho = \frac{2\pi V_{P_1-P_2}}{I}\left[\frac{1}{\left(\frac{1}{r_1}-\frac{1}{r_2}\right)-\left(\frac{1}{r_3}-\frac{1}{r_4}\right)}\right] \quad (3.7)$$

Thus, we can measure the current, voltage, and appropriate distances and solve for resistivity using Schlumberger as shown in figure 3.3

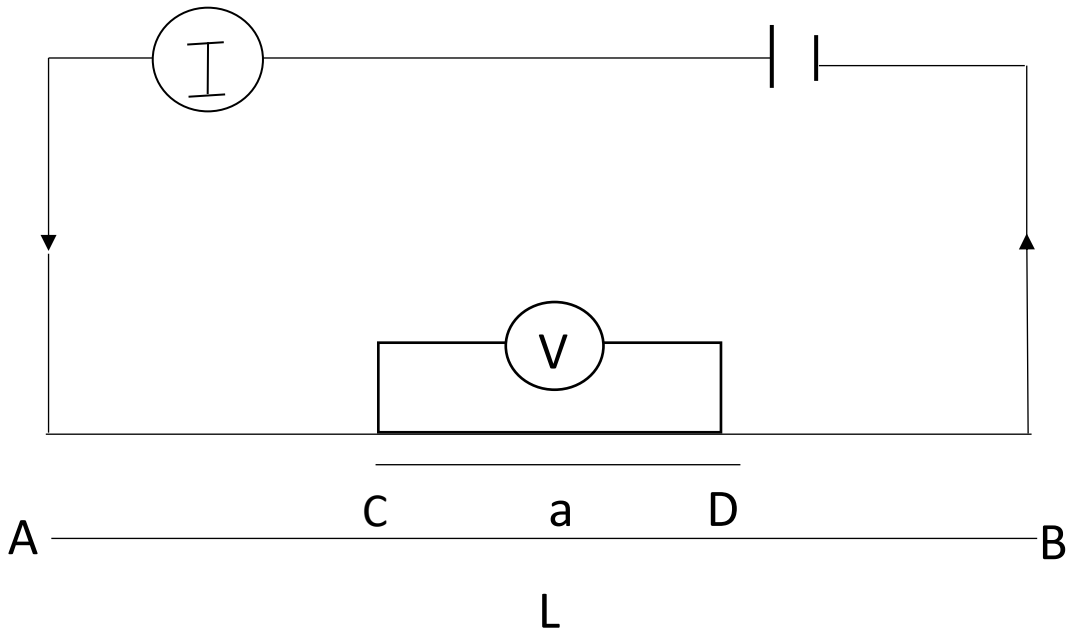

Figure 3: Schlumberger Configuration (Telford, 1990)

The current and potential pair of electrodes in figure 3 often has a common mid-point, but the distances between adjacent electrodes differ. Let the separations of the current and potential electrodes be L and a, respectively.

Then $r_1 = r_{AC} = r_{DB} = r_4 = (\frac{L-a}{2})$ and $r_2 = r_{AD} = r_{CB} = r_3 = (\frac{L+a}{2})$.

Putting these values into equation 3.7, we get:

$$\rho = \frac{2\pi V_{P_1-P_2}}{I}\left[\left(\frac{2}{L+a}-\frac{2}{L-a}\right)-\left(\frac{2}{L+a}-\frac{2}{L-a}\right)\right]^{-1}$$

$$= \frac{\pi V_{P_1-P_2}}{4I}\left(\frac{L^2-a^2}{a}\right) \quad (3.8)$$

Then, the apparent resistivity (ρ_a) values will be obtained by multiplying K with resistance (R) values. i.e.

$$\rho_a = KR \quad (3.9)$$

In addition to currents electrodes A and B, figure 3.4 shows a pair of electrodes M and N which carry no current, but between which the potential difference V may be measured.

The geometric factor (K) in metres is calculated as a function of electrode configuration adopted, for Schlumberger array using figure 3.4.

$$K = \pi\left(\frac{\left(\frac{AB}{2}\right)^2-\left(\frac{MN}{2}\right)^2}{MN}\right) \quad (3.10)$$

where AB is the inter-current electrode spacing and MN is the inter-potential electrode spacing.

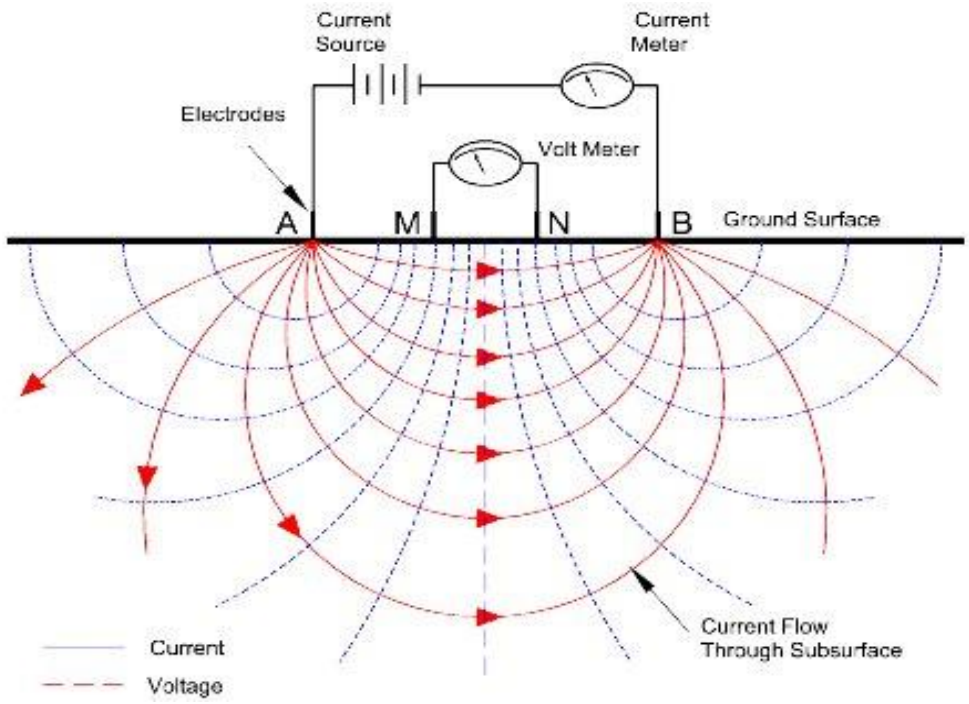

Figure 4: Equipotentials and current lines for a pair of currents electrodes A and B on a homogeneous half-space.

During sounding, apparent resistivity of the subsurface material would be measured as a function of depth. The progressive increase in the distance between the current electrodes will cause the current lines to penetrate to greater depth.

Geometric effects will be renewed from the Pseudo-section and to produce an image of true depth and true formation resistivity, the observed data will undergo a form of processing Known as inversion. For the present work, data will be collected in 2-D using the ABEM SAS 4000 system. The 2-D resistivity imaging survey will be conducted using the Wenner-Alpha electrode array with 5 m electrode spacing.

3.4.1 General Field Procedure for Resistivity Surveys

Regardless of the specific electrode configuration employed, there are really two basic procedures in resistivity work. The particular procedure to be used depends on whether one is interested in resistivity variations with depth or with lateral extent.

The first is called electrical trenching, mapping or horizontal profiling also known as Constant Separation Technique (CST). The second is the electrical drilling, also known as vertical electrical sounding (VES) or (Depth sounding). The directional vertical electric sounding also known as azimuth vertical electrical sounding was used to determine anisotropic properties of subsurface fracture pattern. The electrical resistivity imaging is a powerful tool to investigate subsurface lithologies and structures. It has many advantages over depth sounding or electrical trenching (Ayolabi *et al.,* 2009). This method together with vertical electrical sounding was used in this project

(a) Vertical Electrical Sounding

In vertical electrical sounding (VES) technique, measured vertical variations in the ground apparent resistivity are measured with respect to a fixed Centre of array. This type of survey is carried out by gradually expanding the electrode spacing about a fixed Centre of the array. The Schlumberger arrays are commonly used but the dipole-dipole array could also be used. The presence of horizontal or gently dipping beds of different resistivities is best detected by the expanding spread (Kearey *et al.,* 2002). Hence, the method is useful in determining depth of overburden; define the horizontal strata and resistivity of flat-lying sedimentary beds and possibly of the basement. Vertical electrical sounding (VES) using Schlumberger arrays were used in this project research.

3.4.2 Data Acquisitions

In this study the data collected were basically from main measuring mode of the Terameter SAS 4000 (Resistivity). The profiling data were collected using Schlumberger method of electrical sounding (VES data). Care was taken to ensure that the electrode layout follow a straight line along the N-S profile layout.

Similarly, the maximum current electrode separation of 100m and potential electrode separation of 5m were reached and this corresponds to 50m probed depth (i.e. AB/2).There was no need for data reduction or repeated measurement since the receiver of SAS 4000 discriminates noise and measures voltages corrected with transmitted signal current. The system has the built-in function to average the best measurement of maximum of four staking with the standard deviation of unity or even less (ABEM instrument AB, 1999). The apparent resistivity data were generated from resistance values, using ρ_a=KR. where R= the resistance and K=is the geometric factor. A total of 12 VES points were sounded in both dump site and control site. Win-resist software was used to interpret the data. This particular software performs automatic interpretation of the Schlumberger sounding curves which then gives the equivalent numbers of n-layer model input from the apparent resistivity data of particular sounding VES point.

3.4.3 Geophysical survey curves (electrical sounding curve)

The objective of VES is to obtain a resistivity model (curve) of the subsurface. This is achieved by plotting apparent resistivity obtained for each reading as a function of electrode spacing (AB/2) on a log-log graph sheet with the former on the y-axis and the later on the x-axis.

Inathree layered geo-electric sections, fourstandard curves may be generated as follows:

1. The H- type: is a curvewherehigher resistivity is generated in the shallow soil layers, lower resistivity at moderate depths corresponding to the weathered zone and higher resistivity at depth.It is given by the relation; $\rho_1>\rho_2<\rho_3$.
2. The A- type is a curvewherelower resistivity is generated in the shallow soil layers, higher resistivity at moderate depths and highest resistivity at depth.It is given by the relation where; $\rho_1<\rho_2<\rho_3$.
3. The k- type is a curvewhereby resistivity generated from the shallow soil layers are lower than those at moderate depths and resistivity at depth are lower than those layers above them.It is given by the relation;$\rho_1<\rho_2>\rho_3$.
4. The Q- type is a curve where higher resistivity is generated in the shallow soil layers, low resistivity at moderate depths corresponding to the weathered zone and lower resistivity at depth. It is given by the relation; $\rho_1>\rho_2>\rho_3$.

IV. RESULT

4.1 Results of Vertical Electrical Sounding

Figures 5, 6 and 7 are geoelectric sections (VES curves) where resistivities, depths and thickness of the subsurface were obtained and summarized in Table 3. Others are presented as appendix.

Figure 5 (VES 1) shows the three curve layer indicating H-curve type with configuration$\rho_1>\rho_2<\rho_3$. The resistivity of first layer is 332.1 Ωm to the depth of 1.3 m with the thickness of 1.3 m is an indication that the layer might be lateritic. The resistivity of second layer is 6.3Ωm less than resistivity of first layer to the depth 9.0 m with the thickness of 7.7m is an indication that the layer might be clay. This is interpreted as possible polluted layer due to leachate infiltration from the dumpsite. The resistivity of third layer is 889.6 Ωm which is described as the competent layer that is free from contamination.

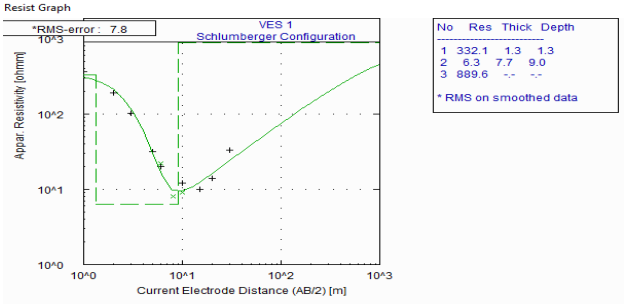

Figure 5: Typical VES Curve along Profile 1 (Dumpsite)

Figure 6 (VES 2) shows that the curve in this profile is characterised to be a three layer model indicating K-curve type with configuration $\rho_1<\rho_2>\rho_3$.The resistivity of first layer is 56.8 Ωm to the depth of 0.4 m with the thickness of 0.4 m is an indication that the layer might be underlain by clay lithology composed of leachate. The resistivity of second layer is 1895.2 Ωm to the depth of 1.3 m with the thickness of 0.9 m is an indication of fresh basement lithology. It is evident that this layer is free from leachate contaminations due to high resistivity value.

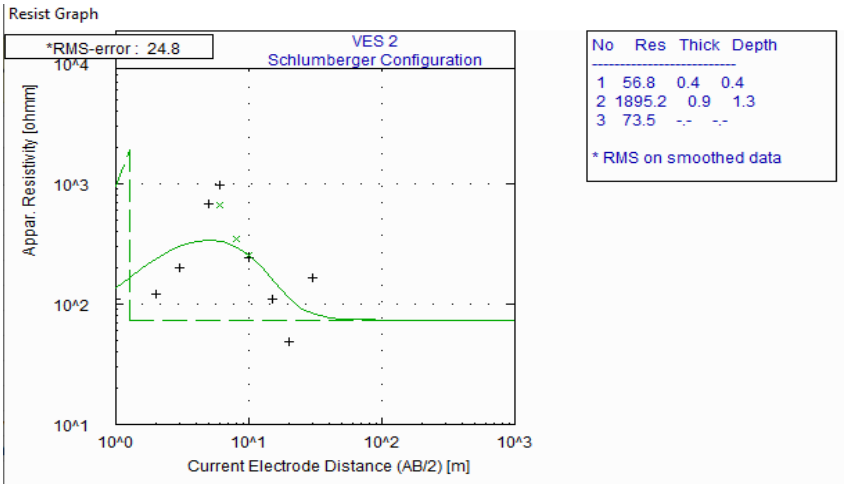

Figure 6: Typical VES Curve along Profile 2 (Dumpsite)

Figure 7 (VES 4) shows that the VES curve in this profile is characterised to be a three layer curve indicating A-curve type with configuration $\rho_1<\rho_2<\rho_3$. The resistivity of first layer is 15.6Ωm to the depth of 3.2 m with the thickness of 3.2 m is an indication that the layer might be underlain by clay lithology composed of leachate due to low resistivity value. The resistivity value of the second layer is 30.2 Ωm to the depth of 14.5 m with the thickness of 11.3 m was interpreted as lateritic soil which underlain the clay material. This moderate resistivity value shows that the leachate is likely present in this layer. The resistivity of the third layer is 7823.4 Ωm which is described as the competent layer that is free from contamination.

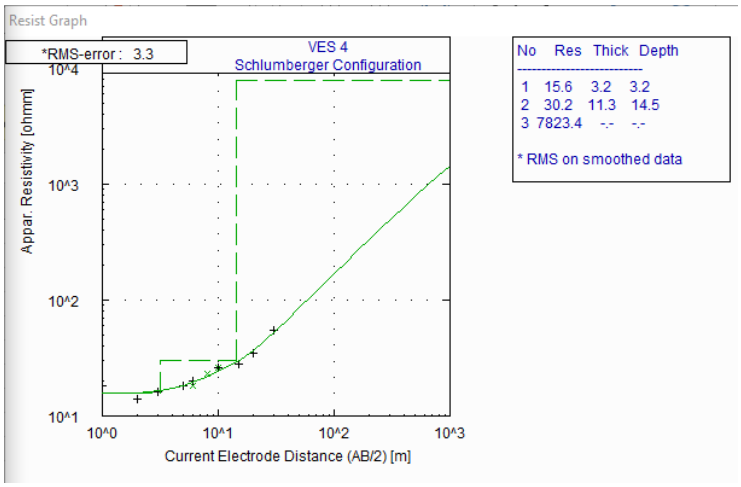

Figure 7: Typical VES Curve along Profile 4 (Dumpsite)

4.2 Interpretation of other VES Curves in Appendix

4.2.1 VES 3: Typical VES curve along profile 3 (dumpsite)

The VES curve in this profile is characterised to be three layer model indicating H-curve type with configuration $\rho_1>\rho_2<\rho_3$. The resistivity of first layer is 559.2 Ωm to the depth of 0.4 m with the thickness of 0.4 m is an indication of unsaturated subsurface

lithology that is free from leachate contamination. The resistivity of the second layer is 6.0 Ωm to the depth of 6.3 m with the thickness of 5.8 m is an indication that the layer might be underlain by clay lithology composed of leachate. The resistivity of the third layer is 3754.7Ωm with the thickness and the depth at infinity. It is evident that this layer is free from leachate contamination.

4.2.2 VES 5: Typical VES curve along profile 5 (dumpsite)

The three curve layer indicating H-curve type with configuration $\rho_1>\rho_2<\rho_3$. The resistivity of the first layer is 103.5Ωm to the depth of 1.0 m with the thickness of 1.0 m is an indication that the layer is weathered basement. The resistivity value of the second layer is 3.8Ωm to the depth of 1.8 m with the thickness of 0.8 m is an indication that the layer might be underlain by clay lithology infiltrated by leachate. The resistivity of the third layer is 35.1Ωm which represent weathered basement attributed to migration of leachate and prone to contamination.

4.2.3 VES 6: Typical VES curve along profile 6 (Dumpsite)

The VES curve in this profile is characterised by a three layer curve indicating H-type with configuration $\rho_1>\rho_2<\rho_3$. The resistivity of first layer is 24.8Ωm to the depth of 0.9 m with the thickness of 0.9 m indicating that the resistivity represents a layer where leachate likely be infiltrated. The resistivity of the second layer is 13.5 Ωm to the depth of 5.9 m with the thickness of 5.1 m indicating that the layer might be underlain by clay lithology composed of leachate. The resistivity of the third layer is 9703.8Ωm which is higher than resistivities of first and second layers is indicative of weathered basement which represents uncontaminated subsurface.

4.2.4 VES 7: Typical VES curve along profile 7 (dumpsite)

The VES curve in this profile is characterised by a three curve layer indicating H-curve type with configuration $\rho_1>\rho_2<\rho_3$. The resistivity of first layer is 463.2 Ωm to the depth of 0.8 m with the thickness of 0.8 m is an indication of weathered lateritic. This layer is defined by unsaturated subsurface with less or no contamination due to high resistivity value. The resistivity of the second layer is 17.3 Ωm to the depth of 11.7 m with the thickness of 10.9 m is an indication of lateritic soil which may likely be infested by leachate. The resistivity of the third layer is 1834.9 Ωm is an indication of fresh laterite that is free from leachate contamination.

4.2.5 VES 8: Typical VES curve along profile 8 (dumpsite)

This is three curve layer indicating H-curve type with configuration $\rho_1>\rho_2<\rho_3$.The resistivity of first layer 123.4 Ωm to the depth of 0.7 m with the thickness of 0.7 m is an indication of lateritic soil with the minimal infiltration of leachate. The resistivity of the second layer is 19.4 Ωm to the depth of 9.9 m with the thickness of 9.2 m is attributed to clay lithology composed of leachate. The resistivity of the third layer is 3309.5Ωm is an indication of fresh lateritic that is free from leachate contamination.

4.2.6 VES 9: Typical VES curve along profile 9 (Dumpsite)

This is three curve layer indicating the H-curve type with configuration $\rho_1>\rho_2<\rho_3$.The resistivity of first layer is 118.5Ωm to the depth of 1.1 m with the thickness of 1.1 m is an indication of weathered basement. The resistivity of the second layer is 19.2 Ωm to the depth of 9.9 m with the thickness of 8.9 m is an indication that the layer might be underlain by clay lithology composed of leachate. The resistivity of the third layer is 5029.5 Ωm. This layer is free from leachate contamination.

4.2.7 VES 10: Typical VES curve along profile 10 (control site)

This is three curve layer indicating H-curve type with configuration $\rho_1>\rho_2<\rho_3$. The resistivity of first layer is 767.1Ωm to the depth of 1.8 m with the thickness of 1.8 m is an indication of weathered lateritic. This layer is free from leachate contamination. The resistivity of the second layer is 11.4Ωm to the depth of 10.2 m with the thickness of 8.4 m is an indication that the layer might be underlain by clay lithology composed of leachate. The resistivity of the third layer is 878.9Ωm is an indication of weathered lateritic. This layer is free from contamination.

4.2.8 VES 11: Typical VES curve along profile 11 (control site)

The four curve layer indicating KH-curve type with configuration $\rho_1<\rho_2>\rho_3<\rho_4$. The resistivity of first layer is 281.6Ωm to the depth of 0.5 m with the thickness of 0.5 m is an indication of weathered basement. The resistivity of the second layer is 936.2 Ωm to the depth of 1.7 m with the thickness of 1.2 m is an indication of fresh lateritic. This layer is free

from leachate contamination. The resistivity of the third layer is 58.0 Ωm to the depth of 17.6 m is an indication that the layer is underlain by clay lithology composed of leachate. The resistivity of the fourth layer is 8007.9 Ωm which is an indication of fresh basement that is free from leachate contamination.

4.2.9 VES 12: Typical VES Curve along Profile 12 (Control site)

The three curve layer indicating H-curve type with configuration $\rho_1>\rho_2<\rho_3$. The resistivity value of first layer is 270.8Ωm to the depth of 1.5 m with the thickness of 1.5 m is an indication of weathered lateritic. The resistivity of the second layer is 6.2Ωm to the depth of 3.7 m with the thickness of 2.1 m is an indication that the layer is underlain by clay lithology or due to migration of leachate. The resistivity of the third layer is 232.5 Ωm which is an indication of weathered basement.

Table 3 shows VES for dumpsite of which VES 1, 3, 5, 6, 7, 8 and 9 are three layers indicating H-curve type with the configuration $\rho_1>\rho_2<\rho_3$. The resistivities of the first layers range from 24.8Ωm – 559.2Ωm. The resistivities of the second layers range from 3.8 Ωm – 19.4Ωm while the resistivity values of the third layers range from 35.1Ωm – 9708.8Ωm. The thickness of the first layers range from 0.4m – 1.3m, the thickness of second layers range from 0.8m – 10.9m, the thickness of third layers are infinity. The depths of first layers range from 0.4m- 1.3m, the depth of the second layers range from 1.8m-11.7m while the third layers are infinity. VES 2 is a three curve layer indicating K-curve type with the configuration $\rho_1<\rho_2>\rho_3$. The resistivity value of the first layer is 56.8Ωm with the thickness of 0.4 m at the depth of 0.4 m. The resistivity value of the second layer is 1895.2 Ωm with the thickness of 0.9 m at the depth of 1.3 m. The resistivity of the third layer is 73.5 Ωm with the thickness and the depths at infinity. VES 4 is a three curve layer indicating A-curve type with the configuration $\rho_1<\rho_2<\rho_3$. The resistivity of the first layer is 15.6 Ωm with the thickness of 3.2 m at the depth of 3.2 m. The resistivity of the second layer 30.2 Ωm with the thickness of 11.3 m at the depth of 14.5 m. This is attributed to clay lithology composed of leachate The resistivity of the third layer is 7823.4 Ωm with the thickness and depth at infinity. This layer is free from leachate contamination.

TABLE 3: Summary of VES analysis for dump site

VES PT	NO OF LAYERS	TYPES OF LAYER CURVE	AVERAGE RESISTIVITY (Ωm)	LAYER THICKNESS(m)	LAYER DEPTH (m)
	1		332.1	1.3	1.3
VES 1	2	H	6.3	7.7	9.0
	3		889.6	∞	∞
	1		56.8	0.4	0.4
VES 2	2	K	1895.2	0.9	1.3
	3		73.5	∞	∞
	1		559.2	0.4	0.4
VES 3	2	H	6.0	5.8	6.2
	3		3754.7	∞	∞
	1		15.6	3.2	3.2
VES 4	2	A	30.2	11.3	14.5
	3		7823.4	∞	∞
	1		103.5	1.0	1.0
VES 5	2	H	3.8	0.8	1.8
	3		35.1	∞	∞

	1		24.8	0.9	0.9
VES 6	2	H	13.5	5.1	6.0
	3		9708.8	∞	∞
	1		463.2	0.8	0.8
VES 7	2	H	17.3	10.9	11.7
	3		1834.9	∞	∞
	1		123.4	0.7	0.7
VES 8	2	H	19.4	9.2	9.9
	3		3309.5	∞	∞
	1		118.5	1.1	1.1
VES 9	2	H	19.2	8.9	9.9
	3		5029.5	∞	∞

Table 4 shows the control site of which VES 10, 11 and 12 are three and four curve layers respectively indicating H-curve type with the configuration $\rho_1>\rho_2<\rho_3$. The resistivities of first layeatrs range from 270.8-767.1Ωm with the thickness ranging from 0.5m – 1.8m at the depths ranges at 0.5 m – 1.8 m at depths ranges 0.5 m – 1.8 m. The resistivities of the second layers range from 6.2 Ωm – 936.2 Ωm with the thickness ranges at 1.2 m – 8.4 m and the depths range at 1.7 m – 10.2 m. The resistivities of third layers range from 58.0 Ωm – 878.9Ωm with the thickness of 15.8 m at the depth of 17.6 m. The resistivity of fourth layer of VES 11 is 8007.9 Ωm with the thickness and depths at infinity.

TABLE 4: Summary of VES analysis for control site

VES PT	NO OF LAYERS	TYPES OF LAYER CURVE	AVERAGE RESISTIVITY (Ωm)	LAYER THICKNESS(m)	LAYER DEPTH (m)
	1		767.1	1.8	1.8
VES 10	2	H	11.4	8.4	10.2
	3		878.9	∞	∞
	1		281.6	0.5	0.5
VES 11	2	KH	936.2	1.2	1.7
	3		58.0	15.8	17.6
	4		8007.9	∞	∞
	1		270.8	1.5	1.5
VES 12	2	H	6.2	2.1	3.6
	3		232.5	∞	∞

V. DISCURSION

The 2D Earth resistivity imaging obtained along profile 01 is shown in Figure 8. The inverse model of this profile shows a clear disparity between low, moderate and large conductive zone within the subsurface. From the surface to about 6 m depth on the profile, the resistivity response is of a moderate range between 13 and 41Ωm. This is interpreted as unpolluted lateritic soil with a minimal leachate contamination zone observed at (65-70) m on the surface profile distance to the depth of about 6 m. From (0.0-40.0) m distance on the surface profile line, the profile is characterized by low resistivity value range from 2-8Ωm. This is interpreted as possible polluted zone due to leachate infiltration from the dumpsite. From about (45-100) m on the profile, at the depth of 12.0-19.8 m, the profile is characterized with high resistivity value range

from70-131Ωm. This zone is interpreted as unsaturated and unpolluted fresh basement rock.

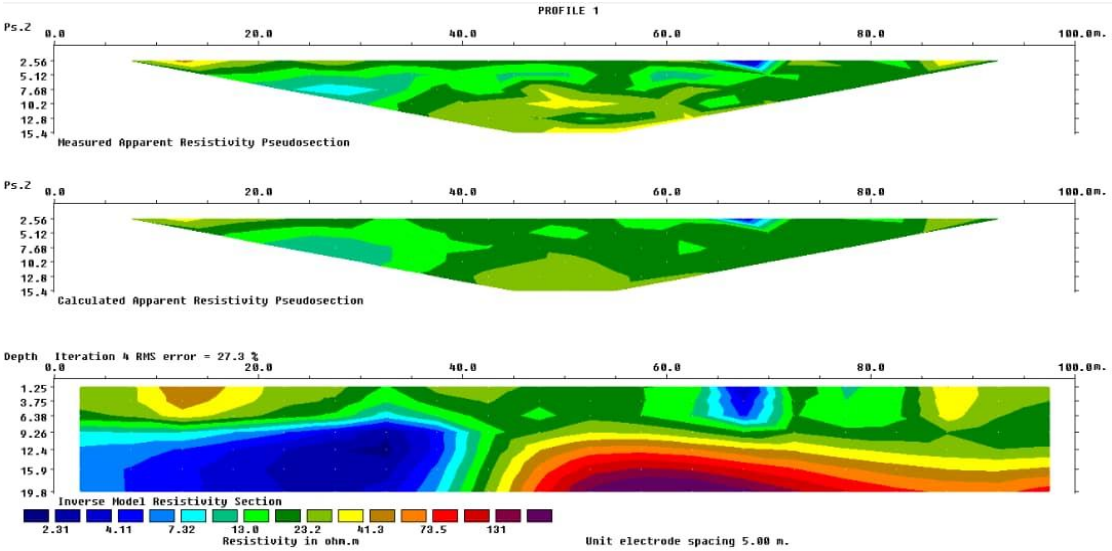

Figure 8: 2D Inverse ERI Plot for Profile 01

At the near subsurface, the 2-D electrical resistivity results obtained (Figure 9) shows a very low resistivity ranges from (17.4-34.9)Ω m at depth of (1.25-7.0) m. Low resistivity behaviour is observed across the profile which suggest a possible infiltration of leachate. Another resistivity values were observed at the depth (9.26-14.0) m which extend from (0.0-100) m with the resistivity values varying from (49.3-98.7) Ωm. This moderate resistivity is an indicative of lateritic soil with minimal infiltration. The third layer represented in the profile is attributed to weathered rock with the resistivity value of (98.7-140)Ωm. The distance ranges from (0.0-20) m at depth of (15.9-19.8) m suggest a possible minimal contamination. It was also observed that resistivity values ranges from (140-198)Ωm from the distance of (40-100) m at the depth of (15.9-19.8) m is an indicative of weathered rock or basement rock. This region is highly resistive to leachate contamination.

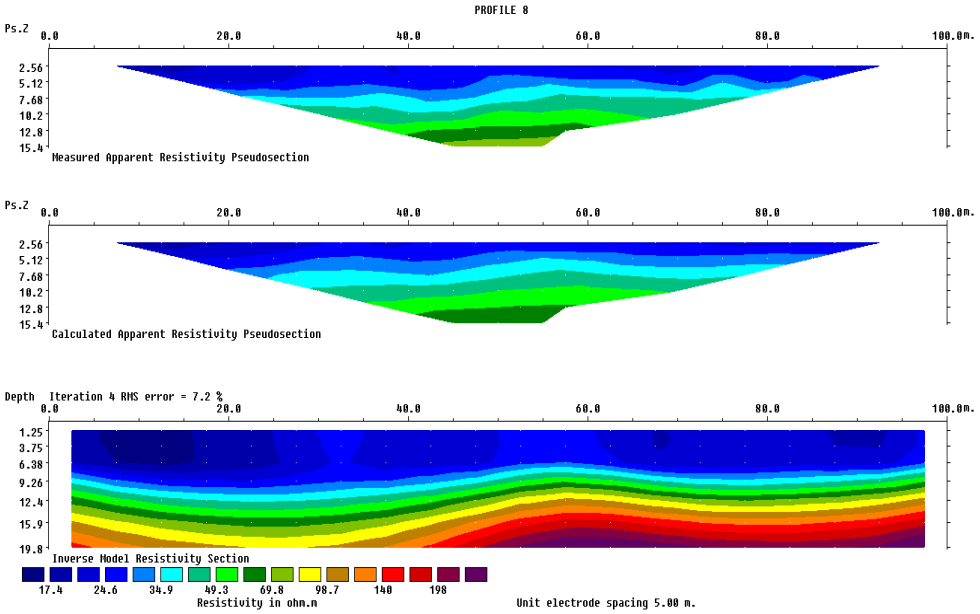

Figure 9: 2D Inverse ERI Plot for Profile 08

The resistivity distribution over a lateral distance of (0.0-100) m at the depth of (1.25-12.4) m and from (15-30) m at the depth of (6.38-12.4) m at the control point revealed enormously low resistivity (5.05-18.6) Ωm in figure 10 is attributed to wet clay and saturated soil. At the shallow subsurface there exist a moderate resistivity values ranges from (35.6-137) Ωm. At lateral distance from (2-68) m which fall within the depth of 6.38 m represents clay lateritic materials which are free from leachate. The low resistivity was also observed from lateral distance of (40-87) m at the depth of (9.26-12.4) m and from (70-75) m at the depth of (3.75-12.4) m with a resistivity of (5.05-18.6) Ω m. The low resistivity observed in this region is an indication of clay material which are also free from contamination since the control point is far from dumpsite. Another moderate resistivity was observed from the distance of (32-100) m at the depth of (2.4-19.8) m with the resistivity values ranges from (35.6-68.3) Ωm. The high resistivity was observed towards the end of the profile from the distance of (85-100) m at the depth of (15.9-19.8) m with the resistivity values ranges from (131-482) Ωm. This portion attributed to weathered rock which is free from contamination.

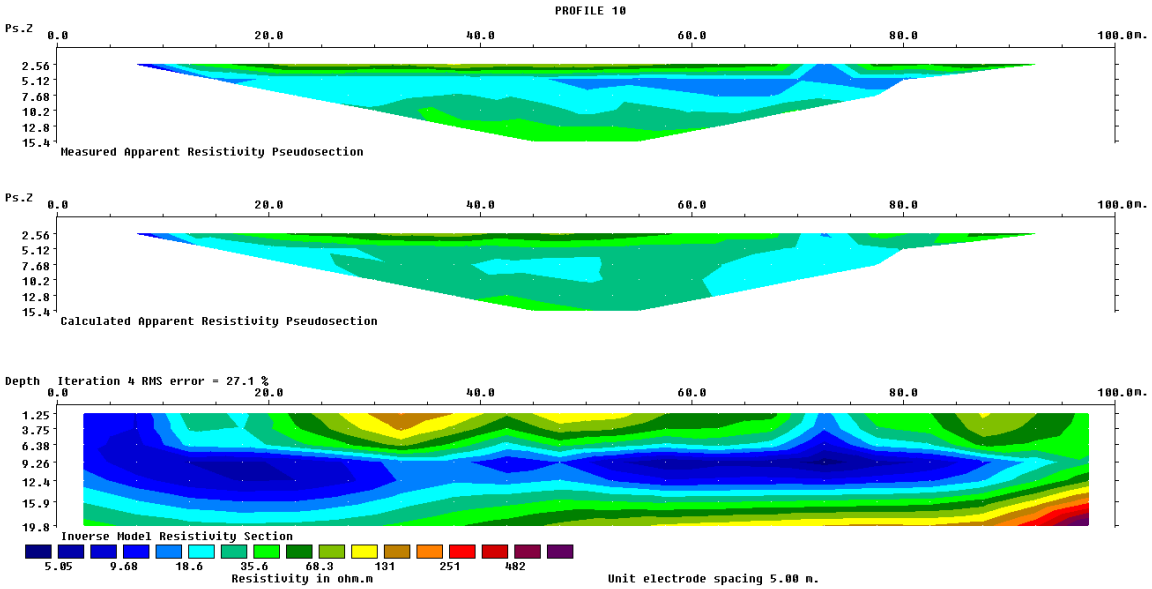

Figure 10: 2D Inverse ERI Plot for Profile 10

5.1 Overburden thickness contour maps

Surfer 10 software package was used to produce the overburden thickness contour maps by contouring the depth values of all the second layers of the entire VES points. The procedure was carried out for both the dump and control sites. The rationale behind contouring is to correlate the two maps and identify the depth of contamination (weathered zone). The deductions made from them are as discussed below.

5.1.1 Deductions from overburden thickness contour map of the dump site

The depth to basement contour map as shown in Figure 11 is contoured at intervals of 0.5 m. The map gives the depth to basement from the surface. The data used to generate the map is the depth values corresponding to the second layer for all the VES points on the dump site.

The contour map reveals the highest depths on the dumpsite which range from 7 m to 14.5 m and are found at VES points 1, 2, 3, 4 and 7 while relatively shallow depth ranging from 1 m to 6 m is revealed at VES points 5, 6, 8 and 9. Overburden thickness contour map shows the pattern of the overburden thickness of the region. The overburden thickness is found at the northwest and western parts of the area, while low overburden thickness is observed at the south, southeast and central portions of the study area

.

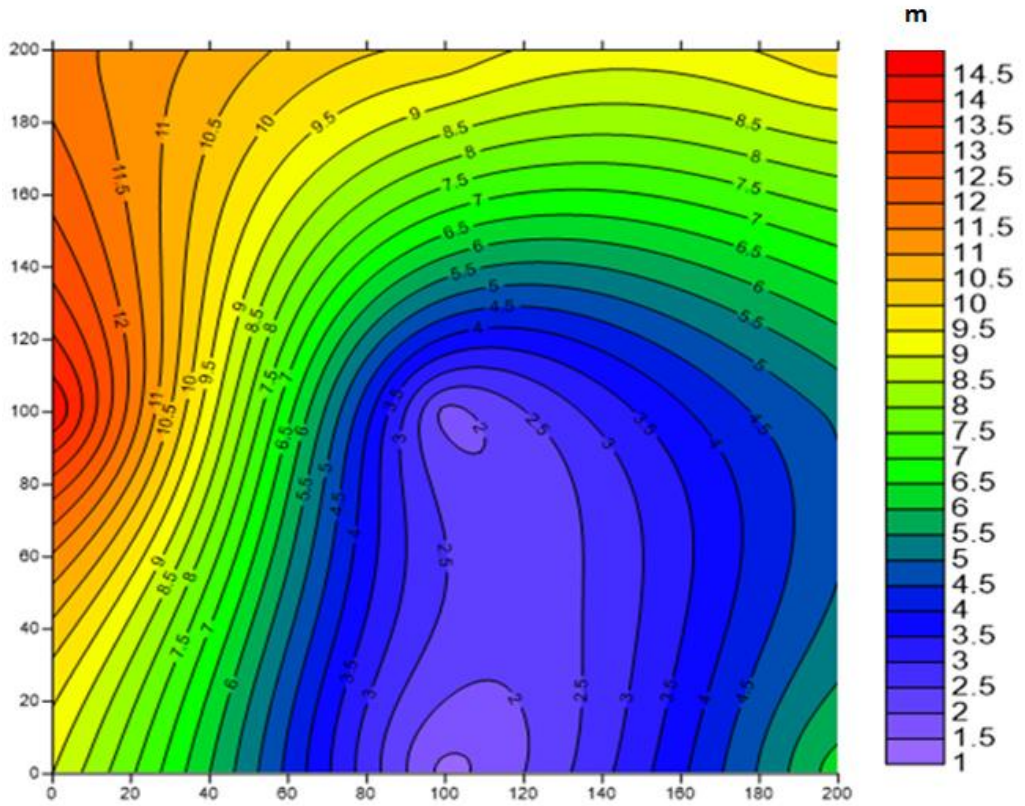

Figure 11: Overburden Thickness Contour Map for Dump Site (Contour Interval of 0.5 m)

5.1.2 Deductions from overburden thickness contour map of the control site (3 VES points)

The depth to basement contour map as shown in Figure 12 is contoured at intervals of 1.0 m. The map gives the depth to basement from the surface. The data used to generate the map are the depth values corresponding to the second layers for all the VES points on the control site. The contour map for the control site reveals that the depth varies from 3.5 m to 17.5 m.

The contour map reveals the highest depth of 17.5 found at VES 11, the average depth of 10 m is found at VES 10 while shallow and least depth of 3.5 m is found at VES 12. Overburden thickness contour map of the control site shows the pattern of the overburden thickness of the area.

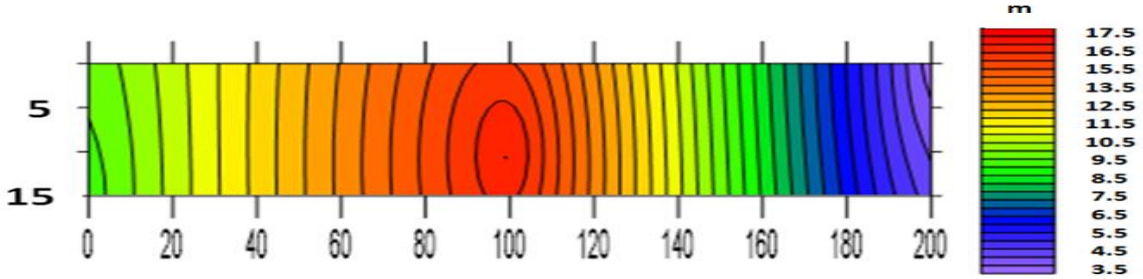

Figure 12: Overburden Thickness Contour Map for Control Site

5.2 Iso-resistivity contour maps at various depths

Iso-resistivity maps in figure 5.6 show the resistivity pattern with depth through slicing of the entire study area horizontally or through a cross-section. Surfer 10 software package was used to produce the contour maps by contouring resistivity values beneath all the VES points at various depths of interests which are; 5m, 10m and 15m respectively. The procedure was carried out for the dump site. The deductions made from them are:

5.2.1 Deductions from iso-resistivity map at the 5m depth

Iso-resistivity contour map was produced for the dump site at the depth of 5m. This is to determine the movement of the contaminant at the subsurface. Figure 13 shows the iso-resistivity maps of the dump site at the depth of 5m. The contour interval for the map is 1 Ω. The resistivity value at the dump site ranges from 1 Ωm to 16 Ωm which is very low. The map shows the presence of contaminant on the dump site at the depth of 5m. This is in tandem with the summary of VES analysis presented in Table 4.1 and signifies the gradual down flow of the contaminants.

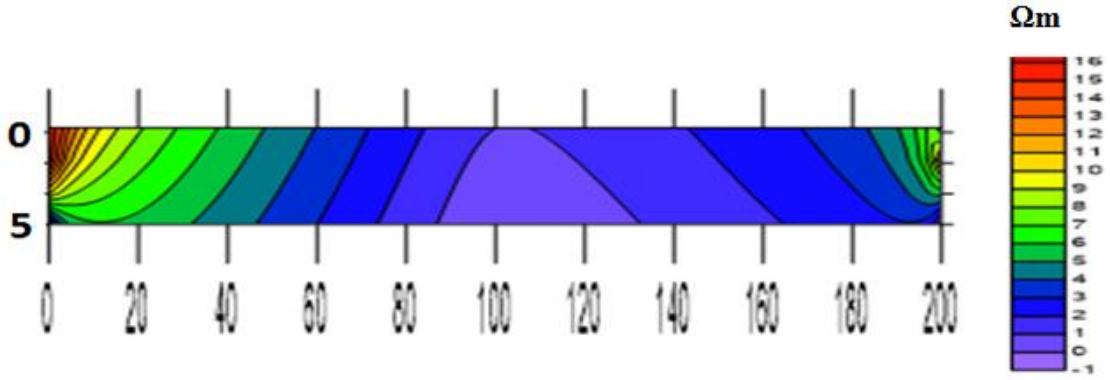

Figure 13: Iso Resistivity Contour Map at 5m

5.2.2 Deductions from iso-resistivity map at the 10m depth

Figure 14 shows the iso-resistivity map of the dump site at the depth of 10m. The contour interval for the maps is 1 Ωm. The map is produced in other to monitor the migration of contaminant to 10m depth. The resistivity value at 10m depths range from 0 Ωm to 20 Ωm, with 0 Ωm to 14 Ωm covering a very large percentage of the total area. The area that lies along the first profile is seen to have high resistivity which is an indication of absence of contaminant on that profile. The presence of relatively low resistivity values indicates the migration of contaminants to the depth of 10m on the dump site.

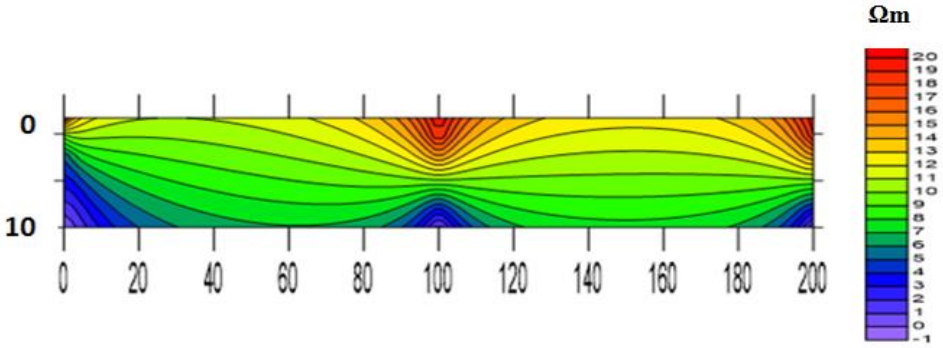

Figure 14: Iso-Resistivity Contour Map at 10 m

5.2.3 Deductions from iso-resistivity map at the 15m depth

Iso-resistivity contour map is produced at the depth of 15m for the dump site. This is to determine the continuous movement of the contaminant at 15 m depth. Figure 15 shows the iso-resistivity map of the dump at 15m. The map is contoured at the interval of 2 Ωm. The resistivity values at 15m depth ranges from 0 Ωm to 32 Ωm. The presence of contaminants seems to have diminished at this level as the highest resistivity values at 15 m depth (32 Ωm) is higher than that of 10 m depth (20 Ωm).

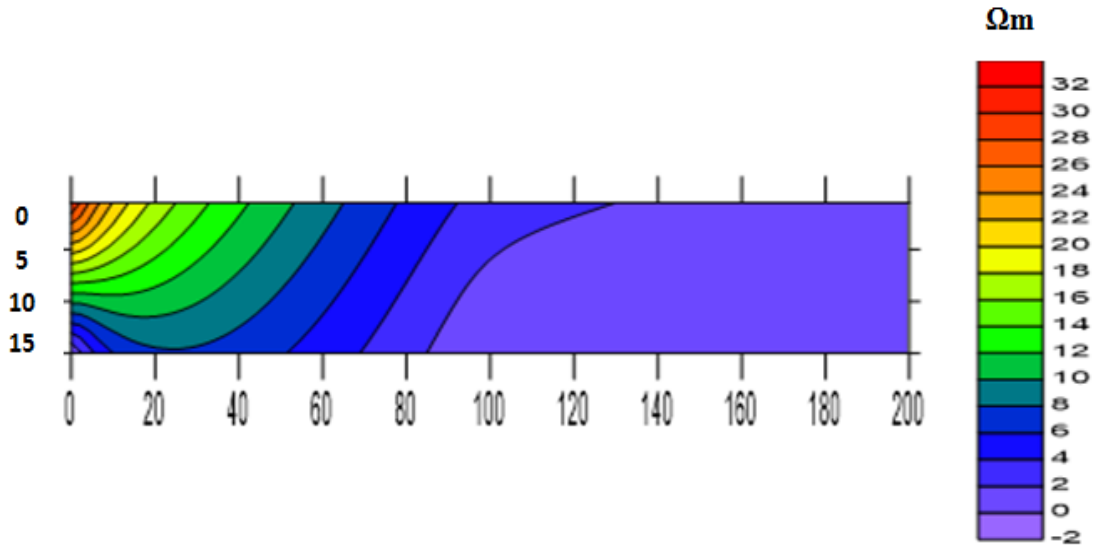

Figure 15: Iso Resistivity Contour Map at 15m

Figures 16, 17 and 18 are geoelectric sections (VES curves) where resistivities, depths and thickness of the subsurface were obtained and summarized in Table 3. Others are presented as appendix.

Figure 16 (VES 1) shows the three curve layer indicating H-curve type with configuration$\rho_1>\rho_2<\rho_3$. The resistivity of first layer is 332.1 Ωm to the depth of 1.3 m with the thickness of 1.3 m is an indication that the layer might be lateritic. The resistivity of second layer is 6.3Ωm less than resistivity of first layer to the depth 9.0 m with the thickness of 7.7m is an indication that the layer might be clay. This is interpreted as possible polluted layer due to leachate infiltration from the dumpsite. The resistivity of third layer is 889.6 Ωm which is described as the competent layer that is free from contamination.

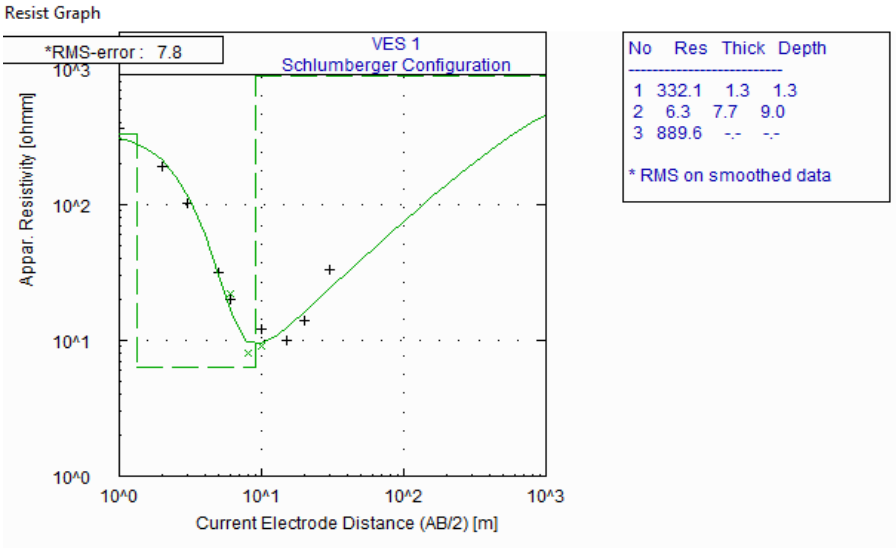

Figure 16: Typical VES Curve along Profile 1 (Dumpsite)

Figure 17 (VES 2) shows that the curve in this profile is characterised to be a three layer model indicating K-curve type with configuration $\rho_1<\rho_2>\rho_3$.The resistivity of first layer is 56.8 Ωm to the depth of 0.4 m with the thickness of 0.4 m is an indication that the layer might be underlain by clay lithology composed of leachate. The resistivity of second layer is 1895.2 Ωm to the depth of 1.3 m with the thickness of 0.9 m is an indication of fresh basement lithology. It is evident that this layer is free from leachate contaminations due to high resistivity value.

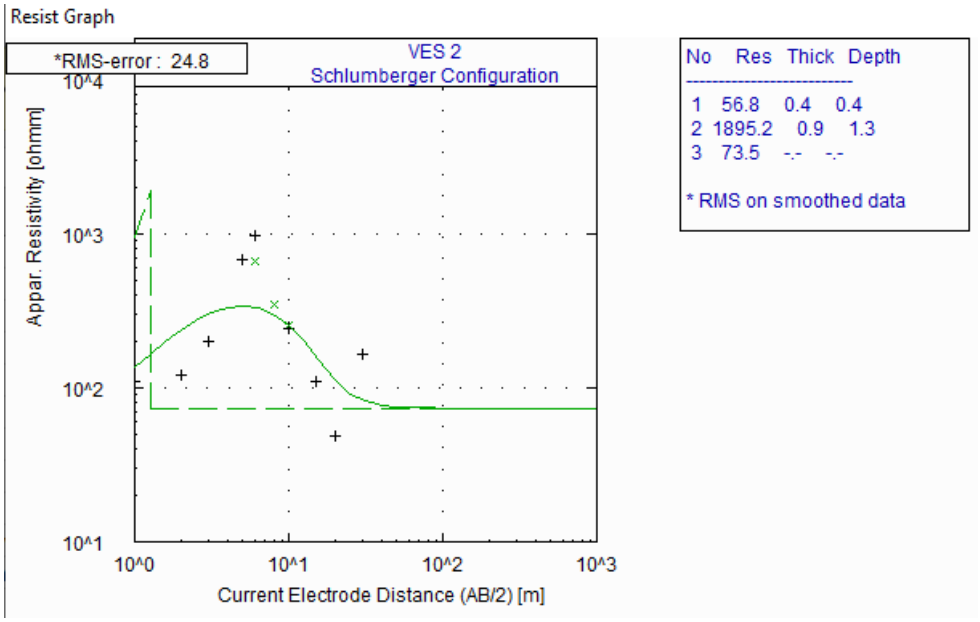

Figure 17: Typical VES Curve along Profile 2 (Dumpsite)

Figure 18 (VES 4) shows that the VES curve in this profile is characterised to be a three layer curve indicating A-curve type with configuration $\rho_1<\rho_2<\rho_3$. The resistivity of first layer is 15.6Ωm to the depth of 3.2 m with the thickness of 3.2 m is an indication that the layer might be underlain by clay lithology composed of leachate due to low resistivity value. The resistivity value of the second layer is 30.2 Ωm to the depth of 14.5 m with the thickness of 11.3 m was interpreted as lateritic soil which underlain the clay material. This moderate resistivity value shows that the leachate is likely present in this layer. The resistivity of the third layer is 7823.4 Ωm which is described as the competent layer that is free from contamination.

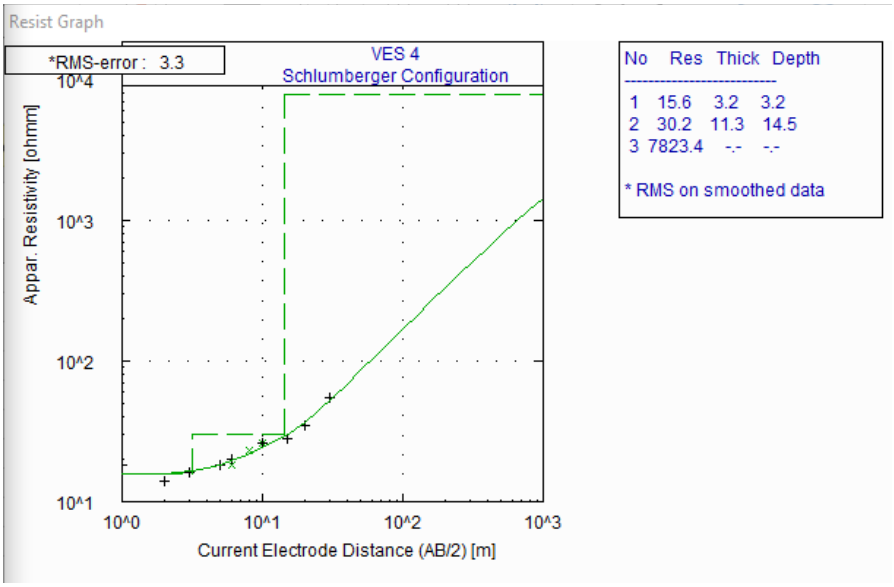

Figure 18: Typical VES Curve along Profile 4 (Dumpsite)

CONCLUSION

Data analysis and the interpretation of this surveying work have indicated the suitability and efficiency of profiling and vertical electrical sounding (VES) methods in probing subsurface structures and delineating level of leachate plume contaminant in basement terrain like Minna. These particular

methods have delineated variations in resistivity in the study area.

The 2-D results revealed three distinctive layers of the subsurface and they are topsoil, weathered rock and the fresh basement. The topsoil comprise of clay and lateritic soil. The resistivity value of (2.3-7.0) Ωm from profile distance (0.0-40) m and from (65-70) m at the depth of (9.0-19.8) m and (1.25-6.38) m respectively as indicated in profile 01 inferred wet clay material while the moderate resistivity (13.0-23.2) Ωm from profile distance of (0.0-5.7) m, (20-25) m, (40-45) m, (50-55) m, (75-100) m at depth (1.25-6.38) m, (1.25-19.8) m and (1.2-12.5) m respectively can be considered as lateritic soil. The conductive zone can be interpreted as polluted zone due to leachate infiltration from the dumpsite while the lateritic soil is referred to zone of minimal leachate contamination. From about (45-100) m on the same profile at the depth (12.0-19.8) m, the profile is characterized with high resistivity values (70-131) Ωm. This zone is interpreted as uplifted weathered basement rock. Profiles 2-9 exhibits similar homogenous resistivity variations. The shallow surface with average resistivity values range from (6.15-40) Ωm within the profile distance of (0.0-100) m at the depth of (1.25-7.00) m while the resistivity value ranges from (39.5-102) Ωm within the profile distance (0.0-100) m at the depth (9.26-19.8) and (7.8-9.56) m are characterized with low to moderate resistivity. The high resistivity value (75-398) Ωm from the profile distance (0.0-100) m, (40-100) m at the depth of (9.26-19.8) m is attributed to weathered rock. Profiles 10-12 represents the control profiles and these profiles exhibits heterogeneous subsurface. The topsoil is characterized with moderate to high resistivity values ranges (27-482) Ωm. The VES results also revealed three different layers which are topsoil, weathered rock and fresh basement. The topsoil comprises of dry loose soil, clay and lateritic soil. The resistivity value (103.5-559.2) Ωm as indicated in VES 11&12 represent the dry loose soil, found at the depth (0.4-1.8) m.

The low resistivity values (3.8-58.0)Ωm with the depth of (3.7-17.6) m are the conductive zone that may likely prone to contamination. The high resistivity observed at the deeper subsurface with values (232.5-9703.8)Ωm at the depth (1.3, 17.6) m is interpreted as weathered rock to fresh basement. The 2-D results revealed the fracture zones as found in profile 1, 10 and 11 with the resistivity values (7.23-35.6) Ωm from the profile distance (30-45) m at the depth of (6.38-19.8) m. The 2-D inversion and the VES results revealed both vertical and lateral electrical resistivity variation with respect to thickness and depth. The low resistivity values range from (2.31-40.0) Ωm at the varying depth as indicated in the 2-D results are inferred as contaminated zones, while the VES results also exhibits low resistivity value (3.8-58.0) Ωm at the varying depths and thicknesses can be interpreted as contamination zone due to leachate penetration.

The 2-D and VES results has successfully delineate the zone of contamination and this is attributed to the region associated with low resistivity value ranging from (3.8-58.0) Ωm which can be interpreted as contaminated zone.

In conclusion, it can be deduced from 2-D and VES results that the area associated with low resistivity is proned to leachate penetration and as such hand dug well is not safe for consumption. The high resistivity can be referred as the competent layer free from leachate infiltration. The low resistivity observed is as a result of leachate contamination which confirm the presence of leachate plume in the study area. Level of leachate contamination of the subsurface was observed on the entire site at varying depths. Fractures observed suggests geological feature that could facilitate leachate plume transport to aquifer or reservoir.

RECOMMENDATION

This research work focus on the uses of two methods, profiling and vertical electrical sounding (VES) on both control and dump site, which also correlated well. It is highly recommended that:

1. The hand dug well should not be constructed in the area, as the area is prone to leachate penetration.
2. The adequate use of refuse collecting methods and enforceable regulations should be established by the government at all level.

REFERENCES

[1]. Alhassan, U.D., Obiora, D.N & Okeke, F.N (2017). Geo-electrical Investigation of Groundwater Potentials of Northern Paiko, Niger State, North Central Nigeria. *Journal of*

Earth Science. 28(1). *Available: http://en.earth-sceince net.*

[2]. Amadi, A. N., Olasehinde, P. I., Obaje, N.O., Unuevho, C.I., Yunusa, M.B., Keke, U., & Ameh, I. M. (2017). Investigating the Quality of Groundwater from Hand-dug Wells in Lapai, Niger State, North-central Nigeria using Physico-chemical and Bacteriological Parameters.*Minna Journal of Geoscience*, 1(1), 77 – 92.

[3]. Amah. O. (2020). Leachate: An Avoidable Threat to Human Health and the Environment. [CCD] AFRICA.

[4]. Anomoharam.(2013). Risk Assessment of Groundwater Contamination. *The Scientific World Journal*. Article ID 610390.

[5]. Carpenter, PJ, Ding. A. & Cheng, L (2012): Identifying Groundwater Continuation Using Resistivity surveys at a landfill. *Department of Geology and Environment Geosciences, Northern Illinois University, Dekalb, IL), Nature Education Knowledge* 3(7): 20

[6]. Cristina, P., Cristina, D., Alicia, F & Pamela, B. (2012). Application of geophysical methods to waste disposal studies, municipal and industrial waste disposal studies. Dr. Xian Ying Yu (Ed) ISBN 978-953-51-0501-5.

[7]. Daniel, G., Bidichael, W.W.E., Ndougsa-Mbarga, T., Kuaiate, K., & Ngoh, J.D. (2011) Hydrogeophysical Investigation for Groundwater Resources from Electrical Resistivity Tomography Self-potential Data in the Meiganga Area, Adamawa, Cameroon. *International Journal of Geo-physics.* Vol/ *Article ID 2697585.*

[8]. Franz, T. (1993). Hydrogeological computer model used in evaluating contaminant transport. *Geotechnical News,* 11(4), pp. 50-52

[9]. Ige, O. O. (2013). Geological and Geotechnical Evaluation of an Open Landfill for Sanitary Landfill Construction in Ilorin, South-western Nigeria.*Journal of Environment and Earth Science*, 3 (3), 9-17.

[10]. Jackson, S (1985). Anatomy & physiology for Nurses. Nurses Aids Senses (9th Ed.) London: Bailliere Tindall.

[11]. Jaglo, K (2002). Groundwater risk analysis in the vicinity of a landfill, a case study in mauritus. M.Sc. Thesis, Royal Institute of Technology, Stockholm.

[12]. Kjeldsen, P, Bartaz M.A, Rooker A.P & Baun* A (2002) Critical review in environmental science and technology 32(4) 297-336.

[13]. Loke, M. H. (1997). Res2DINV software user's manual. *University Sains Malaysia, Penang*.

[14]. Loke, M. H. (2012). Res2dinv ver. 3.71: Rapid 2-d resistivity & IP inversion using the least-squares method. Geotomo software.

[15]. Loke, M.H. (1999). Time-lapse resistivity imaging inversion. Proceedings of the 5th meeting of the Environmental and Engineering Geophysical Society European Section Eml.

[16]. Office of the surveyor general of the federation (OSGOF), Abuja Nigeria (2010). Map of the study area sheet 302 and 303.

[17]. Olawuyi AK & Abolarin SB (2013). Evaluation of Vertical Electrical Sounding Method for Groundwater Development in Basement Complex Terrain of West-Central *Nigeria Journal of Technology Development* Vol.10 No 2

[18]. Ranke, H. G. (2001). Appropriate Design and Operation of Sanitary Landfill in Sustainable Economic Development and Sound Resource Management in Central Asia.Proceedings of an International Conference, Nottingham, United Kingdom.

[19]. Taylor, R & Allen (2006). Waste disposal and landfill. Potential hazard and information needs protecting groundwater for health: managing the quality of drinking-water sources London: IWA publishing.

[20]. Telford. W.M., Geldert, L.P. & Sheriff, R.E. (1990). Applied Geophysics (2nd edition), Cambridge: Cambridge Univ. Press.

[21]. Udensi, E.E., Ogunbanjo, M.I., Nwosu, J.E., Jonah, S.A., Kolo, M.T., Onoduku, U.S., Crown, I.E, Damiyan, M.A., Adeniyi, J.O., & Okosun, F.A (2005). Hydro geological and geophysical surveys for groundwater at designated premises of the main campus of the Federal University of Technology, Minna. *Zuma Journal of Pure and Applied Science* (ZJ PAS). 7(1): 52-58.